THE JOURNAL OF PHYSICAL CHEMISTRY B

Article

pubs.acs.org/JPCB

Radical Cationic Pathway for the Decay of Ionized Glyme Molecules in Liquid Solution

Konstantin S. Taletskiy,[†,‡,⊥] Vsevolod I. Borovkov,[*,†,‡] Lyudmila N. Schegoleva,[§] Irina V. Beregovaya,[§] Andrey I. Taratayko,[‡,§] and Yuriy N. Molin[†]

[†]Voevodsky Institute of Chemical Kinetics and Combustion, Siberian Branch of the Russian Academy of Sciences, 3, Institutskaya str., 630090 Novosibirsk, Russia

[‡]Novosibirsk State University, 2, Pirogova str., Novosibirsk 630090, Russia

[§]Vorozhtsov Institute of Organic Chemistry, Siberian Branch of the Russian Academy of Sciences, 9, Akad. Lavrent'ev Ave., Novosibirsk 630090, Russia

Supporting Information

ABSTRACT: Chemical stability of primary radical cations (RCs) generated in irradiated matter determines substantially the radiation resistance of organic materials. Transformations of the RCs of the glyme molecules, $R(-O-CH_2-CH_2-)_nO-R$ ($R = CH_3$, $n = 1-4$) has been studied on the nanosecond time scale by measuring the magnetic field effects in the recombination fluorescence from irradiated liquid solutions of the glymes. In all cases, the RCs observed were different from that expected for the primary ones and revealed very similar hyperfine couplings independent of the poly(ethylene oxide) chain length and of the substitution of terminal methyl groups by C_2H_5 or CH_2CH_2Cl, as has been shown with diglyme as an example. Quantum chemical analysis of possible chemical transformations for the monoglyme RC as a model system allowed us to discover the reaction pathway yielding the methyl vinyl ether RC. The pathway involves intramolecular proton transfer followed by C−O bond cleavage. Only one ($-O-CH_2-CH_2-O-$) fragment is involved in this transformation, which is nearly barrierless due to the catalytic effect of adjacent glyme molecules. The rapid formation of the methyl vinyl ether RC in the irradiated monoglyme was confirmed by the numerical simulation of the experimental curves of the time-resolved magnetic field effect. These findings suggest that the $R'-O-CH{=}CH_2^{\bullet+}$ formation is a typical decay pathway for the primary RCs in irradiated liquid glymes.

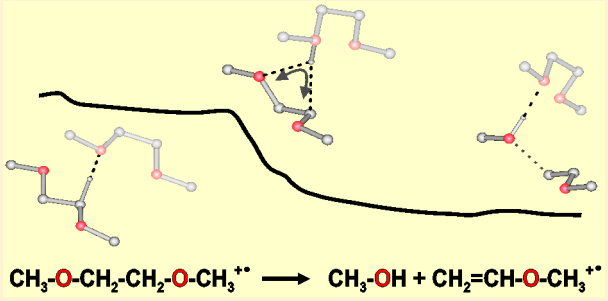

1. INTRODUCTION

Organic saturated compounds typically have ionization potentials sufficiently high to prevent the formation of their radical cations (RCs) in thermal, electrochemical, or photochemical reactions. However, RCs of such compounds can be generated using high-energy radiation. Understanding the pathways of chemical transformations of these RCs is critical for improving the radiation resistance of the compounds. This paper presents a study of radical cationic species arising upon the irradiation of liquid acyclic glymes (ethylene glycol dimethyl ethers), $R(-O-CH_2-CH_2-)_nO-R$. It is of importance for applications of these substances as the electrolyte components of lithium batteries,[1] which can be exploited in a high-energy radiation environments like space or nuclear power plants. Similar cyclic compounds, crown ethers, are used for the extraction of radioactive metal cations from liquid nuclear waste, and the radiation stability of the extracting agent is of considerable importance (e.g., see ref 2 and references therein). Very recently, it was proposed to simulate the aging of electrolytes in Li-ion batteries using high energy radiation.[3] Undoubtedly, an adequate model of the processes in the irradiated electrolytes should take into account the involvement of possible radical cationic species.

Note that the primary RCs and excess electrons generated in organic liquids by ionizing radiation are initially separated by several nanometers. Therefore, the probability for these pairs to recombine is high, resulting in short lifetimes even for chemically stable RCs. This typically prevents them from being observed using conventional EPR techniques in liquid solutions, so matrix isolation techniques are commonly used (e.g., see refs 4 and 5).

Pulsed radiolysis experiments with liquid glymes used as solvents were focused on studying solvated electron (e.g., see refs 6 and 7) or secondary ions (e.g., see ref 8). Radiation studies of glyme related radicals were carried out in low-temperature matrices in order to stabilize the radiolytically generated products. In irradiated frozen solution of the monoglyme (1,2-dimethoxyethane) in $CFCl_3$ at 77 K, Symons

Received: June 25, 2015
Revised: October 9, 2015
Published: October 15, 2015

ACS Publications © 2015 American Chemical Society

DOI: 10.1021/acs.jpcb.5b06086
J. Phys. Chem. B 2015, 119, 14472−14478

and Wren[9] observed a radical with an EPR spectrum that corresponded to the isotropic hyperfine coupling (HFC) constant $a(10H) \approx 1$ mT. This HFC was attributed to the protons in the monoglyme RC.

On the other hand, authors of refs 10 and 11 reported that the EPR spectrum observed in the irradiated frozen monoglyme as well as monoglyme in freon matrices does not exhibit any signal from the primary RC. The EPR spectrum observed at 77 K in the monoglyme solutions in $CFCl_3$ revealed a triplet with a HFC of about 2 mT. This spectrum was attributed to $ROCH_2^{\bullet}$ radicals, in particular, to a distonic RC, $CH_3{-}OH^{+}{-}CH_2{-}CH_2{-}O{-}CH_2^{\bullet}$. Perhaps this should be present as the products of the intramolecular proton transfer. When the temperature increased, the EPR spectrum changed to a 1:4:1 superposition of the ESR spectra from three postulated radical species: $CH_3{-}OH^{+}{-}CH_2{-}CH_2^{\bullet}$, $CH_3{-}O{-}CH{=}CH_2^{\bullet+}$, and $CH_3{-}O{-}CH^{\bullet}{-}CH_2{-}O{-}CH_3$.[10]

In irradiated liquid solutions of spin traps in the monoglyme, adducts of spin-traps with the products of RC transformation have been observed in place of that with the primary RC.[11] In particular, the EPR spectrum obtained in the *tert*-nitroisobutane solution in the monoglyme at $T = 293$ K was attributed to the adducts with $C^{\bullet}H_2{-}O{-}CH_2{-}CH_2{-}O{-}CH_3$, $CH_3{-}O{-}C^{\bullet}H{-}CH_2{-}O{-}CH_3$, and $CH_3{-}O{-}CH{=}CH_2^{\bullet+}$ radical species.

A study of the monoglyme RC decomposition in the gas phase suggested[12] that the most favorable reaction for the isolated RC was the methyl alcohol elimination yielding the methyl vinyl ether RC, $CH_3{-}O{-}CH{=}CH_2^{\bullet+}$. The postulated decay includes three sequential intramolecular H atom transfers, a, b, and c (the maximum barrier is about 10 kcal/mol), followed by the C−O bond cleavage as shown in Scheme 1.

Scheme 1. Sequence a, b, c of Intramolecular Transfers: 1−5, 4−1, 5−2 in the Monoglyme RC

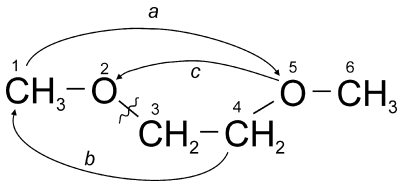

Thus, transformations of the primary RCs of glymes involving intra- and intermolecular transfers of a proton or an H atom yield a variety of neutral radicals and radical cations, including distonic ones. These free radicals were studied either indirectly with spin trapping in liquids or on a comparatively long time scale with the steady-state EPR technique in low temperature matrices.[13] Note that the neutral radicals were investigated in more detail compared with the less stable radical cations, the study of which demands an approach with a high time resolution. To the best of our knowledge, there are no data on the glyme RCs transformation to the radical cationic products on the nanosecond time scale.

To address this issue for liquid glymes, we used the technique of time-resolved magnetic field effect (TR MFE) in the recombination fluorescence.[14,15] This technique probes the radical ions providing information on the spin-correlated radical ion pairs, whose recombination results in the electronically excited states of luminescent molecules. Such pairs are generated by the ionizing irradiation, and importantly, the chemical transformation of a radical ion to another radical ion does not change the spin correlation between the pair partners. It allows focusing on the radical cationic pathway of the primary RC transformation, that is, the pathway along which the positive charge and unpaired electron spin can be considered as remaining unseparated. If charge and spin were separated via an irreversible intermolecular proton transfer then no fluorescence sensitive to external magnetic fields would be expected.

The TR MFE method is in close connection with the EPR method[14,15] yielding the spectroscopic information on HFC constants and *g*-values for the radical ions having very short lifetime.[15,16] Previously, the TR MFE technique was used to establish the structure and explore the dynamics of alkane RCs in liquid solutions.[17,18] Recently, RCs in ionized liquid tetrahydrofuran[19] and monoglyme[20] have been detected using this technique; however, the nature of those RCs was not recognized.

2. METHODS AND MATERIALS

2.1. The Approach. In irradiated organic solution, the radical ions that are formed in the early stages of radiolysis are the solvent RC and excess electron. To readily observe the pair recombination luminescence and isolate the features related to the RCs, we need to scavenge electrons with a suitable acceptor. To this end, the scavenger should be a luminophore molecule with a short fluorescence lifetime. Another prerequisite condition is a sufficiently small HFC in the radical anion to slow the decay of the initial spin coherence in the spin-correlated radical ion pairs. That is why we used the dilute glyme solutions of *para*-terphenyl-d_{14} (*p*TP) whose luminescence quantum yield is close to unity and radical anions have negligible HFC constants.

Note that the excess electrons migrate more rapidly than the molecular ions, so they are scavenged typically much faster than the solvent RCs. Therefore, shortly after the irradiation pulse, delayed fluorescence should appear due to the recombination of radical anions of *p*TP with the positive charge carrier $S^{+\bullet}$ resulting from the solvent ionization:

$$S^{+\bullet} + pTP^{-\bullet} \rightarrow S + pTP^{*} \qquad (1)$$

This reaction is expected to determine the fluorescence response until $S^{+\bullet}$ also reacts with *p*TP. Note that $pTP^{-\bullet}$ can also recombine with distonic RCs (see the Introduction) or with closed-shell cations, the possible cationic products of the proton transfer from the glyme RC to a solvent molecule. It seems unlikely, however, that *p*TP* fluorescence can originate from such recombination since those reactions are expected to have insufficient energy to yield electronically excited *p*TP (e.g., see ref 20). On the other hand, Vyushkova et al.[21] ascribed the delayed fluorescence from the irradiated concentrated solutions of 2,2,6,6-tetramethylpiperidine in alkanes to the recombination of radical ion pairs involving the complex between radical cation and neutral molecule, in which the charge and the spin densities were well separated due to the intracomplex proton transfer. Therefore, *a priori* we cannot exclude the contribution of the distonic RCs to the delayed fluorescence from the glyme solutions.

The recombination fluorescence intensity, $I(t)$, is proportional to the yield of singlet excited state of the luminophore via reaction 1. In turn, this singlet state, $^1pTP^*$, appears upon the recombination of the radical ion pair in its singlet state, whose population, $\rho_{SS}(t)$, varies with time due to singlet−triplet transitions. These transitions are driven by the electron spin

DOI: 10.1021/acs.jpcb.5b06086
J. Phys. Chem. B 2015, 119, 14472−14478

interaction with nuclear spins as well as those with an external magnetic field, **B**. Though it could scarcely be justified rigorously, it is believed that in weakly polar solutions the rate, $R(t)$, of the radical ion pair recombination does not show a noticeable dependence on both the spin state of the pair and the external magnetic field. To our knowledge, there is no experimental evidence that argues against this statement. As a result, the fluorescence decay curve, $I(t)$, turns out to be dependent on external magnetic field as follows:

$$I(t) \propto R(t)\rho_{SS}(\mathbf{B}, t) \tag{2}$$

The $R(t)$ dependence cannot be determined independently; thus it is advisible to explore the spin evolution of spin correlated radical ion pairs using the ratio

$$\frac{I_B(t)}{I_0(t)} \approx \frac{\rho_{SS}(\mathbf{B} > 0, t)}{\rho_{SS}(\mathbf{B} = 0, t)} \tag{3}$$

This ratio defines the TR MFE kinetic curve and can be calculated analytically in the limit of strong magnetic field **B**.[14] For zero field, the analytic calculation is possible for radical ions having isotropic HFC with one or two groups of magnetically equivalent protons,[14,15] as well as for radical ions with unresolved EPR spectrum.[22] Otherwise, a numerical solution of the Liouville−von Neumann equation for the spin density matrix $\rho(t)$ is necessary.

2.2. Experimental Details. A series of the glymes, R(−O−CH_2−CH_2−)$_n$O−R (R = CH_3, n = 1−4), and two substituted diglymes (R = CH_2CH_3 or CH_2CH_2Cl) have been examined. We irradiated (1−5) × 10^{-4} M solutions of *para*-terphenyl-d_{14} in these glymes and also in 0.1−1 M solutions of the glymes in *n*-hexane, decane, and squalane (2,6,10,15,19,23-hexamethyltetracosane). Short X-ray pulses having quantum energy of about 20 keV were used to irradiate the samples. The fluorescence response of the system was studied using the single photon counting technique with a time resolution of about 2 ns.[23]

The fluorescence from the irradiated samples was observed in the magnetic field range of 0−1 T. We used the optical filter with the bandpass of 260−390 nm to isolate the *p*TP fluorescence. The temperature dependence of TR MFE was measured in the range 253−333 K (±1 K). Before the experiments, oxygen was removed from the solutions by several freeze−pump−thaw cycles.

In the present work, the TR MFE curves were simulated using the numeric calculation of the $\rho_{SS}(t)$ spin state evolution taking isotropic HFC and Zeeman interactions into account. Paramagnetic relaxation was included as described previously.[14−18] The contribution of the *p*TP radical anion to the spin dynamics was described using a quasiclassical approximation[22] at the width σ = 0.068 mT of the EPR spectrum of the radical anion (e.g., see refs 14 and 15).

2.3. Chemicals. We used 1,2-dimethoxyethane (monoglyme, 99.5%), diglyme (99.5%), triglyme (99%), tetraglyme (99%), di(ethylene glycol) diethyl ether (99%), squalane (99%), *n*-hexane (99%), decane (98%) and *para*-terphenyl-d_{14} (98% D atoms) received from Aldrich. The solvents were additionally purified by a passage through a column with activated alumina and then stored over sodium to keep them dry. The synthesis of 1,11-dichloro-3,6,9-oxo-undecane is described in the Supporting Information.

2.4. Quantum Chemical Calculations. The calculations of the glyme molecules, RCs, and the profiles of potential energy surfaces (PESs) along the pathways of the RC transformations were carried out in the adiabatic approximation using the density functional theory (DFT) with the B3LYP and M06-2X functionals implemented in GAMESS package.[24] The most calculations, including estimation of the HFC constants, were done at the B3LYP/6-31+G* level. In some cases, the M06-2X functional was used, but no significant differences were found. The stationary PES points were located, and their type was determined from the analysis of normal vibrations. The interrelations between the stationary points were established using the intrinsic reaction coordinate (IRC) calculations. The effect of the medium was taken into account using the conductor-like polarizable continuum model (CPCM) built in GAMESS, with tetrahydrofuran as a reference solvent with a dielectric permittivity close to that of glymes.[25]

3. RESULTS AND DISCUSSION

3.1. Time-Resolved Magnetic Field Effects. Figure 1 shows the experimental TR MFE curves for liquid glyme solutions of *p*TP. The curve features in Figure 1 do not change noticeably for different compounds. They remain nearly the same upon the dilution of the glymes by the alkanes down to 0.1 M. No significant temperature variations were observed in the range of 253−333 K.

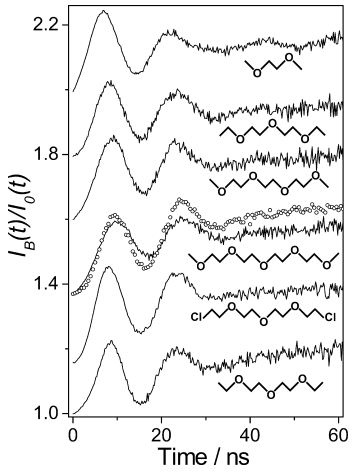

Figure 1. Experimental TR MFE curves, $I_B(t)/I_0(t)$, for solutions of 5 × 10^{-4} M *p*TP in the glymes indicated in the plot in the magnetic field **B** = 0.1 T. The results were obtained at room temperature. For the chlorinated compound, the data obtained with 0.1 M solution in *n*-hexane are given. The data for 0.1 M solution of tetraglyme obtained in squalane at 333 K are indicated with circles. For clarity, the curves are spaced vertically relative to each other.

The features in the curves originate from singlet−triplet oscillations (quantum beats) in the spin-correlated radical ion pairs, $S^{+\bullet}/pTP^{-\bullet}$, that are driven by HFCs in the radical ions. HFC constants in the deuterated radical anion are too small to contribute to the spin evolution before 30−50 ns. Therefore, the appearance of the first TR MFE feature with its maximum at $\tau_1 \approx$ 7−8 ns is determined by the width, σ, of the EPR spectrum of the RC.[14,15] The presence of another feature at $\tau_2 \approx$ 20−23 ns suggests that the number of magnetically equivalent protons with the largest HFC constant in the RC is even.[14,15]

Using the known equations,[14,15,18] one can estimate the second moment, σ^2, of the EPR spectrum of the RC, $\sigma \approx 9/\tau_1(\text{ns}) \approx$ 1.1−1.3 mT, and the largest HFC constant, $a(\text{H}) \approx 36/\tau_2(\text{ns}) \approx$ 1.6−1.8 mT. A more quantitative analysis will be

DOI: 10.1021/acs.jpcb.5b06086
J. Phys. Chem. B 2015, 119, 14472−14478

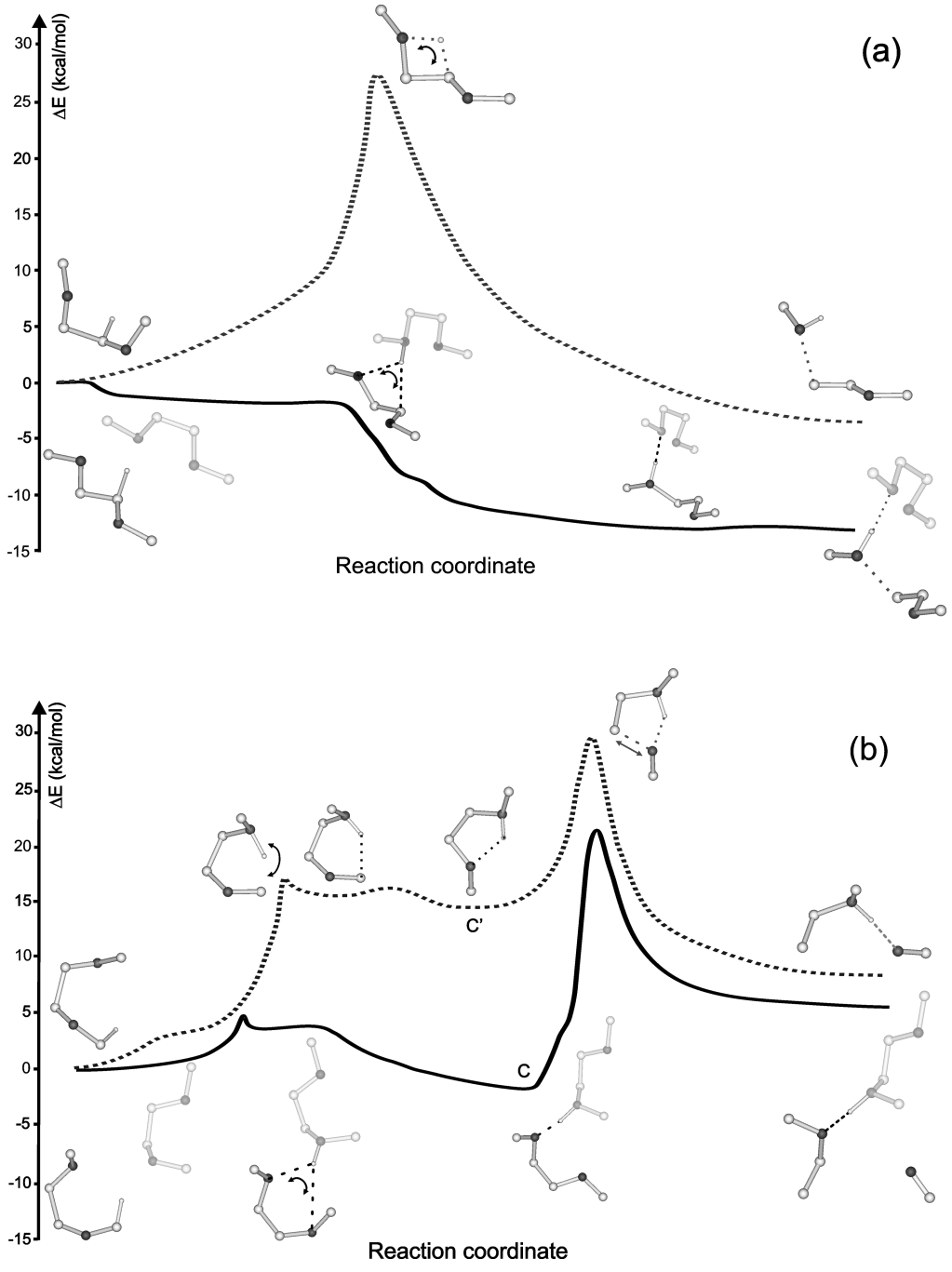

Figure 2. Calculated PES sections along the reaction coordinate for the monoglyme RC conversion to methyl vinyl ether RC (a) and to distonic RC $CH_3{-}OH^+{-}CH_2{-}CH_2^\bullet$ (b). Another distonic RC, $CH_3{-}OH^+{-}CH_2{-}CH_2{-}O{-}CH_2^\bullet$, corresponds to the local minima C and C′ in panel b. The dashed lines indicate the PES profile for the isolated monoglyme RC, and the solid lines indicate that for the complexes of RC and neutral glyme. The structures indicated with two-way arrows are transition states, while other structures correspond to the PES minima. For clarity, hydrogen atoms that are not involved in the transformations are omitted. Oxygen atoms are shown as black spheres.

given below, although even this crude estimate suggests that there are only two protons with significant HFC constants. In the EPR spectra, such RCs would be observed as a triplet with line splitting that is similar to the ones observed in low temperature experiments (see the Introduction). For the solvent RCs, we would expect a greater number of coupled protons due to the rapid conformational dynamics occurring in a liquid solution.

Therefore, the delayed fluorescence observed in our experiments originates from the recombination of pairs involving RCs, which are not the primary ones but which appear on the radical cationic pathway of the primary RCs' decomposition. A relatively large magnitude of the quantum beats in the observed TR MFE curves (Figure 1) allows estimation of an upper limit of the typical generation time of these secondary radical cationic species. The quantum beats pattern would be smeared significantly if the generation time, which determines the incoherent scatter of the starting moments for the beats in particular spin-correlated pairs, were comparable with the rise-up portion of the quantum beats

DOI: 10.1021/acs.jpcb.5b06086
J. Phys. Chem. B 2015, 119, 14472−14478

pattern. This rise-up time is about 7−8 ns, and since the generation time of the secondary RCs should be much shorter, we estimate its upper limit as 1 ns. The very short generation time is also confirmed by the TR MFE simulation results (see below) that were obtained assuming instantaneous formation of the secondary RCs.

Note that in the alkane solutions of glymes the secondary RCs are the same as ones that were observed in the directly ionized glyme molecules, although these RCs are likely to be generated due to the charge transfer from alkane RCs in their ground state. This implies that the highly excited states of the glyme primary RCs are unlikely involved in the reactions, which is apparently facile even in the ground state of the RCs. The shapes of the TR MFE curve are nearly the same in a wide temperature range, which indicates that in the liquid state (as opposed to the gas phase experiments[12]) the conversion of the primary RCs of glymes to the secondary RCs has negligible energy barriers.

The similarity of the TR MFE curves obtained for the compounds having terminal moieties different from the methoxy group (two the lowest curves in Figure 1) suggests also that the observed quantum beats are determined by HFC with protons from one of the (−O−CH_2−CH_2−O−) units of the poly(ethylene oxide) chain after the primary RC undergoes the rapid transformation. Additional argument against the important role of the terminal moieties in the transformation is offered by the similarity of the monoglyme and the tetraglyme solutions, in which the relative content of the ethylene oxide units differs significantly.

3.2. Quantum Chemical Analysis. We restricted our computational analysis to the simplest glyme, that is, 1,2-dimethoxyethane. As was discussed in the Introduction, the most likely products of the primary monoglyme RC decay in the low temperature matrices include the RCs of the methyl vinyl ether, CH_3−O−CH═$CH_2^{\bullet+}$, and two distonic RCs, CH_3−OH^+−CH_2−CH_2−O−$CH_2^{\bullet}$ and CH_3−OH^+−CH_2−$CH_2^{\bullet}$.

Using the DFT calculations, we obtained the sections of the PESs corresponding to the primary monoglyme RC transformations leading to these RCs. The calculations were carried out in two variants. For the first one, the effect of the environment was taken into account using solely the CPCM model. For the second, keeping in mind the possibility of the specific interaction of RC with ether solvent molecules,[19] we included explicitly another glyme molecule in the calculations. The results of the calculations for the isolated monoglyme RC are indicated with the dashed lines in Figure 2a,b; the solid lines in this figure relate to the results for the RC−molecule complexes.

Figure 2a presents the reaction pathway for the primary RC yielding the methyl vinyl ether RC and the methyl alcohol. The process combines the proton transfer from the carbon atom to the remote oxygen atom along the pathway 3−5 (Scheme 2a) followed by the cleavage of the C(4)−O(5) bond.

For the RC-molecule complex, the stationary PES structures located along the reaction coordinate reflect a sequential formation of hydrogen bonds between the migrating proton and oxygen atom of the nearby molecule, first C−H···O and then more energetically favorable O−H···O are formed. Importantly, the process described is accompanied by considerable conformational changes of the glyme molecules.

The distonic RCs appear successively in the pathways shown in Figure 2b. In this case (see Scheme 2b), a proton is transferred from the methyl group (the pathway 1−5) yielding the CH_3−OH^+−CH_2−CH_2−O−$CH_2^{\bullet}$ radical (the points C and C′ in Figure 2b). Then the C(2)−O(3) bond breaks, leading to the dissociation into the CH_3−OH^+−CH_2−$CH_2^{\bullet}$ radical and formaldehyde.

Scheme 2. Proton Transfer in the Monoglyme RC along the Pathway (a) 3−5 Producing the Methyl Vinyl Ether RC or (b) 1−5 Producing Distonic RCs, CH_3−OH^+−CH_2−CH_2−O−$CH_2^{\bullet}$ and, finally, CH_3−OH^+−CH_2−$CH_2^{\bullet}$

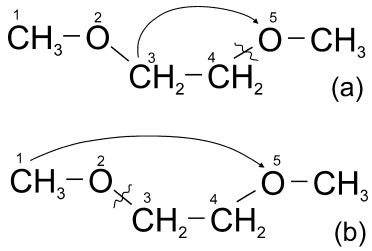

Note that for the isolated RCs, both of the reactions (dashed lines in Figure 2) exhibit significant (∼30 kcal/mol) energy barriers. When another monoglyme molecule is involved, the energy barrier for the formation of the methyl vinyl ether RC disappears (Figure 2a) and the energy barriers on the reaction coordinate leading to the distonic radical cations (Figure 2b, solid line) are dramatically lowered. The first of these barriers (∼4 kcal/mol) relates to the proton transfer from the RC methyl group to the oxygen atom of the same molecule (the 1−5 path, Scheme 2b). This leads to bimolecular complex C (Figure 2b) where the proton is bound to the oxygen atoms of the two glyme moieties. This complex is ca. 10 kcal/mol higher in energy than the complex of the methyl vinyl ether RC and the methyl alcohol. Further transformation of complex C yields another distonic RC, that is, CH_3−OH^+−CH_2−$CH_2^{\bullet}$. Thus, our DFT calculations suggest the dissociation of the monoglyme RC to the methyl vinyl ether RC as the most favorable pathway in solution from both kinetic and thermodynamic points of view.

Note, these results are likely not in disagreement with the experimental yields of the RCs under discussion in low temperature $CFCl_3$ matrix.[10] According to the cited work, the relative yields of the distonic RCs are similar while that of the methyl vinyl ether RC is higher (see the Introduction). The DFT calculations in the present work have been performed taking into account only one additional glyme molecule under the conditions of almost free motion of both particles. In a low temperature matrix, the relative energies of the species involved may be changed arbitrarily due to interaction with several neighboring molecules having unfavorable conformations.

3.3. Simulation of TR MFE Experiments. Experimental and numerically simulated TR MFE curves are shown in Figure 3. Before performing the simulation, we analyzed the HFCs obtained in our calculations for the methyl vinyl ether RC and the first of the distonic RCs, that is, the complex corresponding to point C in Figure 2b. The calculated structures of these RCs are shown in Figure 4, together with the HFC constants.

One can see that for both species, there are two α-protons with HFC constants that are close to each other. For the methyl vinyl ether RC, the estimated HFC constants are ca. −1.7 mT, which agree well with the EPR estimations of −1.87 mT.[26] Calculated HFC constants for other protons are $a'(H_\alpha) \approx -0.3$ mT and $a''(3H) \approx 0.8$ mT (for the magnetically equivalent protons in the methoxy group). In complex C (see

DOI: 10.1021/acs.jpcb.5b06086
J. Phys. Chem. B 2015, 119, 14472−14478

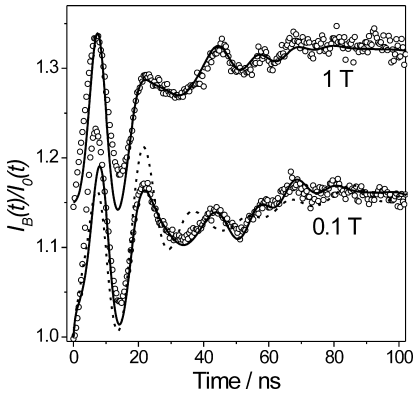

Figure 3. Experimental TR MFE curves, $I_B(t)/I_0(t)$, for the monoglyme containing 5×10^{-4} M *p*TP at **B** = 0.1 T and **B** = 1 T (circles). The solid lines indicate the numerical simulation obtained using the HFC constants $a(2H) = -1.64$ mT, $a'(3H) = 0.58$ mT, and $a''(1H) = -0.29$ mT for the RC. Dashed line is the simulated trace for $a(2H) = -1.7$ mT, $a'(2H) = 0.4$ mT. The difference between the *g*-values of radical ion pair partners equals $\Delta g = 1.0 \times 10^{-3}$; the EPR spectrum width of the *p*TP radical anion equals to 0.068 mT.

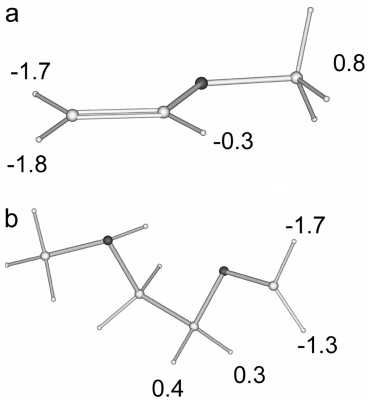

Figure 4. Calculated structures and the larger HFC constants (in mT) for the methyl vinyl ether RC (a) and for the complex C (b) shown without the neutral monoglyme molecule. Oxygen atoms are indicated with the filled circles.

Figure 2b), the HFC constants are predicted to be −1.3 and −1.7 mT for the two α-protons and −0.3 and −0.4 mT for two protons of the (−O−CH_2−CH_2−O−) fragment. We assume that in liquid solution at room temperature these constants will be averaged out inside each group due to flipping between equivalent conformations that would give a triplet of triplets in the corresponding EPR spectra.

The above analysis is important since the quantum beats pattern is very sensitive to the presence of magnetic nuclear configuration with zero total magnetic moment. In particular, in the case of magnetically equivalent protons, some peaks on the TR MFE curve are transformed into dips when the number of the protons changes from even to odd.[14,15]

In this respect, the set of HFC constants $a(2H) + a'(3H) + a''(H)$ for the methyl vinyl ether RC differs from the set of $a(2H) + a'(2H)$ for the distonic RC. As shown in Figure 3, the TR MFE curve simulation starting from the set for the methyl vinyl ether RC and assuming that the secondary RCs are generated instantaneously led to good agreement with the experimental traces with the optimal HFC constants similar to those calculated using DFT approach. The agreement is also good at other magnetic fields if the difference between the *g*-values of the RC and *p*TP radical anion was assumed to amount to $\Delta g = 1.0 \times 10^{-3}$.

At the same time, using the expected set of $a(2H) + a'(2H)$ for the distonic RC, we failed to achieve a good quality fit as demonstrated in Figure 3 by dashed line. In this particular simulation, the fit was performed to reproduce the position of the second peak.

3.4. Other Glymes. Thus, our quantum chemical and experimental results show that the RC of methyl vinyl ether is formed in the course of the decay of the primary monoglyme RC. This reaction is rapid because it has a low activation barrier due to the catalytic effect of the oxygen atom of a nearby glyme molecule. Based on these data and keeping in mind the similarity of the TR MFE curves observed for various glymes (see Figure 1), we can assume that the RCs formed by the fragmentation of the primary RCs of other glyme molecules are the RCs of corresponding vinyl ethers, R−O−CH═$CH_2^{\bullet+}$. The fragmentation involves only the atoms of one (−O−CH_2−CH_2−O−) moiety. Note that for longer glyme molecules one cannot exclude the catalytic effect of the oxygen atom of another ethylene oxide unit of the same glyme RC along with that of a neighboring glyme molecule.

4. CONCLUSIONS

Using the TR MFE method, we showed that radical cations of the acyclic glymes (poly(ethylene glycol) diethers) rapidly (<1 ns) dissociate in liquid solutions. For the monoglyme RC, the quantum chemical analysis of possible decomposition channels revealed a nearly barrierless decay pathway yielding the methyl vinyl ether RC and the methyl alcohol molecule. This reaction channel involves the proton transfer from the methylene group of the glyme to the oxygen atom across the ethylene oxide unit followed by C−O bond cleavage. In both processes, the oxygen atom of a neighboring glyme molecule is involved. The rapid formation of the methyl vinyl ether RC is strongly supported by our simulation of the experimental TR MFE. The similarity of the experimental results obtained for the different glyme compounds suggests that the R′−O−CH═$CH_2^{\bullet+}$ formation is a typical radical cationic decay pathway for the primary RCs in liquid glymes.

At the same time, it should be emphasized that the TR MFE technique is sensitive only to those radical cations that appeared on the radical cationic pathway of the primary RC transformation. In particular, this method can give no evidence for possible parallel channels of the neutral radical formation by any mechanism. Hence, we cannot estimate the actual yield of the RC studied to compare our results with data of EPR studies. The significance of the radical cationic pathway in the decomposition of the irradiated glymes can be recognized using the pulse radiolysis method applied to liquid glymes with isolating the characteristic optical absorption of alkyl vinyl ether RCs in UV range.[27]

The absence of a noticeable energy barrier and the local nature of the primary RC decomposition reaction in the liquid glymes suggest that it may be difficult to preclude the decomposition using concurrent reactions with charge acceptors added to the glymes. A possible way to improve the radiation resistance of these compounds could be the substitution of the (−O−CH_2−CH_2−O−) moiety with a more branched fragment to prevent the proton transfer, or using fragments with a lower ionization potential to minimize the localization of the positive charge on poly(ethylene oxide) chain.

DOI: 10.1021/acs.jpcb.5b06086
J. Phys. Chem. B 2015, 119, 14472−14478

■ ASSOCIATED CONTENT

Supporting Information

The Supporting Information is available free of charge on the ACS Publications website at DOI: 10.1021/acs.jpcb.5b06086.

Description of the synthesis of 1,11-dichloro-3,6,9-oxo-undecane (PDF)

■ AUTHOR INFORMATION

Corresponding Author

*E-mail: borovkov@kinetics.nsc.ru.

Present Address

[⊥]K.S.T.: Center for Molecular Study of Condensed Soft Matter, Illinois Institute of Technology, Suite 150, 3440 S. Dearborn Street, Chicago, Illinois 60616, USA.

Notes

The authors declare no competing financial interest.

■ ACKNOWLEDGMENTS

The work was supported by RFBR (Grant No. 14-03-00570) and by the Council for Grants of the President of the Russian Federation for State Support of Leading Scientific Schools (Grant NSh-5744.2014.3). We gratefully acknowledge all the referees for valuable comments and are indebted to one of them for careful reading our manuscript and for his useful suggestions.

■ REFERENCES

(1) Schaefer, J. L.; Lu, Y.; Moganty, S. S.; Agarwal, P.; Jayaprakash, N.; Archer, L. A. Electrolytes for High-Energy Lithium Batteries. *Appl. Nanosci.* **2012**, *2*, 91−109.

(2) Shkrob, I. A.; Marin, T. W.; Dietz, M. L. On the Radiation Stability of Crown Ethers in Ionic Liquids. *J. Phys. Chem. B* **2011**, *115*, 3903−3911.

(3) Ortiz, D.; Steinmetz, V.; Durand, D.; Legand, S.; Dauvois, V.; Maître, P.; Le Caër, S. Radiolysis as a Solution for Accelerated Ageing Studies of Electrolytes in Lithium-Ion Batteries. *Nat. Commun.* **2015**, *6*, 6950.

(4) Lund, A., Shiotani, M., Eds. *Radical Ionic Systems. Properties in Condensed Phases*; Kluwer Academic Publishers: Dordrecht, The Netherlands, 1991.

(5) Lund, A., Shiotani, M., Eds. *Applications of EPR in Radiation Research*; Springer International Publishing: Cham, Switzerland, 2014.

(6) Seddon, W. A.; Fletcher, J. W.; Sopchyshyn, F. C.; Catterall, R. Solvated Electrons and the Effect of Coordination on the Optical Spectra of Alkali Metal Cation-Electron Pairs in Ethers. *Can. J. Chem.* **1977**, *55*, 3356−3363.

(7) Jou, F. Y.; Dorfman, L. M. Pulse Radiolysis Studies. XXI. Optical Absorption Spectrum of the Solvated Electron in Ethers and in Binary Solutions of These Ethers. *J. Chem. Phys.* **1973**, *58*, 4715−4723.

(8) Solar, S.; Getoff, N.; Haenel, M. W.; Richter, U.-B. Radiation-induced C-C Bond Cleavage in 1,2-Diarylethanes as Model Compounds of Coal. Part 2.-Pulse and Steady-State Radiolysis of 1,2-Di(pyren-l-yl)ethane in Tetrahydrofuran, Dimethoxyethane and Toluene in the Presence of Sodium Dihydrido-bis(2-methoxyethoxy)-aluminate. *J. Chem. Soc., Faraday Trans.* **1993**, *89*, 891−903.

(9) Symons, M. C. R.; Wren, B. W. Electron Spin Resonance Spectra of Ether Radical Cations Generated by Radiolysis. *J. Chem. Soc., Perkin Trans. 2* **1984**, *11*, 511−522.

(10) Baranova, I. A.; Belevskii, V. N.; Belopushkin, S. I.; Feldman, V. I. EPR Study of Reactions of Methylal and Dimethoxyethane Cation Radicals in Condensed Phase. *High Energy Chem.* **1991**, *25*, 450−457.

(11) Belevskii, V.; Belopushkin, S.; Baranova, I.; Tyurin, D. A. Selectivity of Fragmentation and Rearrangements of Ether Radical Cations in the Liquid-Phase Radiolysis. *High Energy Chem.* **1999**, *33*, 379−389.

(12) Thissen, R.; Alcaraz, C.; Dutuit, O.; Mourgues, P.; Chamot-Rooke, J.; Audier, H. A Hidden Hydrogen Transfer in the Unimolecular Reaction of 1,2-Dimethoxyethane$^{\bullet+}$. *J. Phys. Chem. A* **1999**, *103*, 5049−5054.

(13) Feldman, V. I. EPR and IR Spectroscopy of Free Radicals and Radical Ions Produced by Radiation in Solid Systems. In *Applications of EPR in Radiation Research*; Lund, A., Shiotani, M., Eds.; Springer International Publishing: Cham, Switzerland, 2014; pp 151−187.

(14) Bagryansky, V. A.; Borovkov, V. I.; Molin, Y. N. Quantum Beats in Radical Pairs. *Russ. Chem. Rev.* **2007**, *76*, 493−506.

(15) Borovkov, V.; Stass, D.; Bagryansky, V.; Molin, Y. Study of Spin-Correlated Radical Ion Pairs in Irradiated Solutions by Optically Detected EPR and Related Techniques. In *Applications of EPR in Radiation Research*; Lund, A., Shiotani, M., Eds.; Springer International Publishing: Cham, Switzerland, 2014; pp 629−663.

(16) Borovkov, V. I.; Beregovaya, I. V.; Shchegoleva, L. N.; Blinkova, S. V.; Ovchinnikov, D. A.; Gurskaya, L. Y.; Shteingarts, V. D.; Bagryansky, V. A.; Molin, Y. N. Structure and Stability of Pentafluoroaniline and 4-Aminononafluorobiphenyl Radical Anions: Optically Detected Electron Paramagnetic Resonance, Time-Resolved Fluorescence, Time-Resolved Magnetic Field Effect, and Quantum Chemical Study. *J. Phys. Chem. A* **2015**, *119*, 8443−8451.

(17) Potashov, P. A.; Borovkov, V. I.; Shchegoleva, L. N.; Gritsan, N. P.; Bagryansky, V. A.; Molin, Y. N. Radical Cations of Branched Alkanes in Solutions: Time-Resolved Magnetic Field Effect and Quantum Chemical Studies. *J. Phys. Chem. A* **2012**, *116*, 3110−3117.

(18) Borovkov, V. I.; Bagryansky, V. A.; Yeletskikh, I. V.; Molin, Y. N. Radical Cations of n-Alkanes in Irradiated Solutions as Studied by Time-Resolved Magnetic Field Effects. *Mol. Phys.* **2002**, *100*, 1379−1384.

(19) Taletskiy, K.; Borovkov, V.; Shchegoleva, L.; Beregovaya, I.; Bagryansky, V.; Molin, Y. Unusual Transformation of Primary Radical Cations in Irradiated Liquid Tetrahydrofuran. *Dokl. Phys. Chem.* **2014**, *455*, 41−44.

(20) Borovkov, V. I.; Ivanishko, I. S. Measurement of the Relative Mobility of Geminate Ions in Ethereal Solutions of Aromatic Compounds Using the Fluorescence Response of the Solutions to Pulsed Irradiation. *J. Phys. Chem. B* **2013**, *117*, 15122−15130.

(21) Vyushkova, M. M.; Borovkov, V. I.; Shchegoleva, L. N.; Beregovaya, I. V.; Bagryanskii, V. A.; Molin, Yu. N. Unusual Proton-Transfer Complex between the 2,2,6,6-Tetramethylpiperidine Radical Cation and Neutral Molecule. *Dokl. Phys. Chem.* **2008**, *420* (2), 125−127.

(22) Schulten, K.; Wolynes, P. G. Semiclassical Description of Electron Spin Motion in Radicals Including the Effect of Electron Hopping. *J. Chem. Phys.* **1978**, *68*, 3292−3297.

(23) Anishchik, S. V.; Grigoryants, V. M.; Shebolaev, I. V.; Chernousov, Yu. D.; Anisimov, O. A.; Molin, Yu. N. Pulsed X-ray Fluorometer with Nanosecond Resolution. *Prib. Tekhn. Eksp. (Russ.)* **1989**, *4*, 74−79.

(24) Schmidt, M. W.; Baldridge, K. K.; Boatz, J. A.; Elbert, S. T.; Gordon, M. S.; Jensen, J. H.; Koseki, S.; Matsunaga, N.; Nguyen, K. A.; Su, S. J.; et al. General Atomic and Molecular Electronic Structure System. *J. Comput. Chem.* **1993**, *14*, 1347−1363.

(25) Wohlfarth, C. Static Dielectric Constants of Pure Liquids and Binary Liquid Mixtures. Supplement to IV/6. *Landolt-Börnstein. Numerical Data and Functional Relationships in Science and Technology, Group IV Physical Chemistry*; Lechner, M.D., Ed.; Springer: Berlin, 2008.

(26) Knolle, W.; Janovský, I.; Naumov, S.; Mehnert, R. Low-temperature EPR Study of Radical Cations of Vinyl Ethers in a Freon Matrix. *Radiat. Phys. Chem.* **1999**, *55*, 625−631.

(27) Pankasem, S.; Rosenau-Eichin, R.; Thomas, J. K.; Weiss, D. Pulse Radiolysis of Vinyl Monomers, in the Pure State and with Added Pyrene. *Radiat. Phys. Chem.* **1996**, *47*, 827−833.

DOI: 10.1021/acs.jpcb.5b06086
J. Phys. Chem. B 2015, 119, 14472−14478